

See discussions, stats, and author profiles for this publication at: <https://www.researchgate.net/publication/307126573>

Evaluation of High-Temperature Oxidation Behavior of Inconel 600 and Hastelloy C-22

Dataset · August 2016

CITATIONS

0

3 authors, including:



Ali Sabea Hammood

University Of Kufa

75 PUBLICATIONS 20 CITATIONS

SEE PROFILE

Evaluation of High-Temperature Oxidation Behavior of Inconel 600 and Hastelloy C-22

Ammar Abdulkareem Hashim¹ · Ali Sabea Hammood² · Nawal Jasem Hammadi¹

Received: 19 January 2015 / Accepted: 10 June 2015 / Published online: 30 June 2015
© King Fahd University of Petroleum & Minerals 2015

Abstract The aim of this study was to investigate the oxidation behavior of nickel-base superalloys (Inconel 600 and Hastelloy C-22) by the determination of the oxidation rates of alloys at elevated temperatures and at ambient air. The cyclic oxidation method was adapted by heating of alloys periodically in still air at 900, 1000 and 1100°C followed by cooling at ambient temperature. The weight change measurement was recorded during the cyclic oxidation tests. The X-ray diffraction and microstructure study were also used as characterization methods to illustrate the properties of studied alloys and oxide film that formed on the surface of oxidized alloys. Inconel 600 and Hastelloy C-22 showed their ability to develop a uniform protective oxide film. The oxide film that formed on both alloys was chromia oxide Cr_2O_3 with smaller amount of spinel oxide NiCr_2O_4 . The results of the weight gain measurements suggest that the oxidation kinetics of both alloys follows the parabolic behavior during the experimental tests. Also both alloys at 1100°C exhibited severe spallation of oxide film with linear decreasing in the weight change measurements. The p-kp model was implemented to describe the subsequent cyclic process of oxide growth and spalling.

Keywords High temperature oxidation · Nickel-base alloys · Weight gain measurements · P-kp model

✉ Ammar Abdulkareem Hashim
ammamsc11@yahoo.com

Ali Sabea Hammood
alis.altameemi@uokufa.edu.iq

Nawal Jasem Hammadi
drnawaleng@yahoo.com

¹ Engineering College, Basra University, Basra, Iraq

² Faculty of Engineering, Kufa University, Najaf, Iraq

1 Introduction

Nickel-base superalloys are very complex structure materials because typically contain more than ten different alloying elements and intended to produce a combination of high-temperature strength to elevated temperatures and resistance to corrosion. These alloys are primarily used in gas turbines, coal conversion plants and chemical process industries, and for other specialized applications requiring heat and/or corrosion resistance [1,2].

Many of the nickel superalloys in the high-temperature environments are oxidized in air or in other high oxidizing environments. High-temperature oxidation of many of these materials often resulted in the formation and growth of a continuous external oxide scale and/or in the internal oxidation of the less-noble constituents of the oxidized materials. Heat-resisting alloys are commonly classified as chromia-forming or alumina-forming alloys according to the nature of the protective oxide scale formed up on their high-temperature oxidation. However, Cr_2O_3 grows on the Ni-base alloys when containing at least 1, Wt% Cr for the chromia-forming alloys [3].

Many components experience cyclic oxidation in applications that entail periodic start-up and shutdown. Typically, some scale spallation may occur upon cooling, resulting in the loss of the protective diffusion barrier provided by a fully intact scale [4]. Cyclic oxidation testing has therefore been a mainstay of material characterization and performance ranking for high-temperature materials. The engineering response is generally characterized non-destructively by weight change curves and surface recession [4]. Generally, cyclic oxidation weight change curves exhibit a basic shape consisting of an initial weight gain to a maximum value, a decrease followed by crossover to negative weight changes and finally a nearly linear rate of weight loss [5]. Many

researchers conducted to study oxidation resistance of nickel-base superalloys; Huang studied the oxidation behavior and mechanism of a new type of wrought Ni–Fe–Cr–Al superalloys and compared with Haynes 214, Inconel 600 and GH 3030 in the temperature range of 1100–1300 °C [6]. G. Mori investigated thermogravimetric effect in air under isothermal conditions for Hastelloy C-22, Nimonic 80A and Hastelloy N [7]. The oxidation behavior of Ni-20Cr-coated and uncoated nickel superalloys at an elevated temperature of 900 °C in air was studied by Singh [8]. The humidity influence on the high-temperature oxidation of Inconel 600 was investigated in the thermal gravimetric analysis under artificial air between 600 and 900 °C by Xiao [9].

To describe and understand factors affecting cyclic oxidation, mechanistic models have been developed to quantify scale growth and loss in a manner to generate mass change curves similar to those obtained from cyclic oxidation testing [10]. Most important models employed in different investigations are cyclic oxidation spall program (COSP) uniform layer (UL) version, COSP Monte Carlo (MC) version [11, 12], deterministic interfacial cyclic oxidation spall model (DICOSM) [4] and a statistical model developed by Monceau (p-kp model) [13].

Each model operates on the same principle and basic iterative process where oxide forms during the high-temperature segment of the cycle and spallation occurs during the cooling segment. Where these models differ greatly in the approach, each model employs statistically managing oxide spallation during the cooling [10]. In the p-kp model, the oxide scale partly spalls and the spalling probability, p, does not vary with time or space. In the DICOSM, the spalling area fraction is constant and the area that spalls is always the thickest segment of the scale. The COSP-UL simulates a spallation from the entire outer surface as a UL and COSP-MC as discrete segments detached at the interface. This model is based on a randomized probability (Monte Carlo) [14].

The purpose of this work was to study the oxidation behavior of Inconel 600 and Hastelloy C-22 at high temperatures throughout the determination of oxidation rates at ambient air, and then, p-kp model was used to predict the oxidation resistance of alloys on the basis of the obtained experimental data.

2 Experimental Procedures

The nominal chemical composition of superalloys Inconel 600 and Hastelloy C-22 used in this study is given by using

Table 1 Chemical composition of studied alloys, Wt%

| Material | Ni | Cr | Mo | Fe | Co | Mn | Cu | Ti | W | Nb |
|----------------|-------|-------|-------|------|------|------|------|------|------|------|
| Inconel 600 | 74.54 | 15.50 | 0.15 | 9.21 | 0.32 | 0.16 | 0.17 | 0.33 | – | – |
| Hastelloy C-22 | 58.84 | 19.51 | 13.49 | 4.89 | 2.09 | 0.27 | 0.06 | – | 2.93 | 0.04 |

spectrometer X-ray tube alloy analyzer, X MET 3000TX, Metorex Inc., Germany, as shown in Table 1.

The Inconel 600 and Hastelloy C-22 alloys were cut into squares specimens with dimensions (20 x 20 x 5 mm), and the total area of exposed was 1200 mm². All specimen surfaces were wet ground using 120-grit alumina papers; then, the specimens were cleaned with acetone and rinsed with distilled water. The surface areas of specimens were measured and then dried and weighed before commencement of the experiments. The oxidation kinetics of nickel alloys was studied by measuring the weight change. The weight gains during the heating of the specimens periodically in still air at 900, 1000 and 1100 °C in an electrical furnace for 1 h, and cooled for half an hour at ambient temperature. After each 1-h cycle of heating and half-an-hour cooling, the specimens were reweighed and then returned to the furnace for the next identical heating cycle as described in Fig. 1 where the T_{max} represents the oxidation temperature and T_{min} represents the ambient temperature. Spalled oxide was not included in the weight measurements. The surfaces of the specimen were brushed before weighing to remove any loose oxide.

The balance that was used had resolution of ±0.1 mg. The net weight change was calculated by the following Eq. 1:

$$\frac{\Delta W}{A} = \frac{W_f - W_o}{S} \quad (1)$$

where the W_f is the weight of specimen after each heating cycle, W_o is the original weight of specimen before the heating cycle, S is the surface area of the specimen. X-ray diffraction (XRD) analyses with optical microscope test were used as characterization methods to determine the oxide composition, oxide morphology and spalls areas.

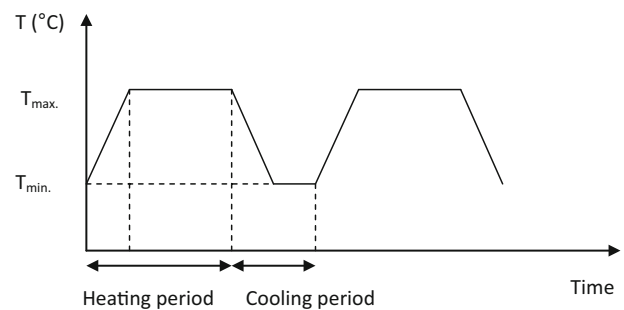


Fig. 1 Sketch of oxidation cycles at high temperature

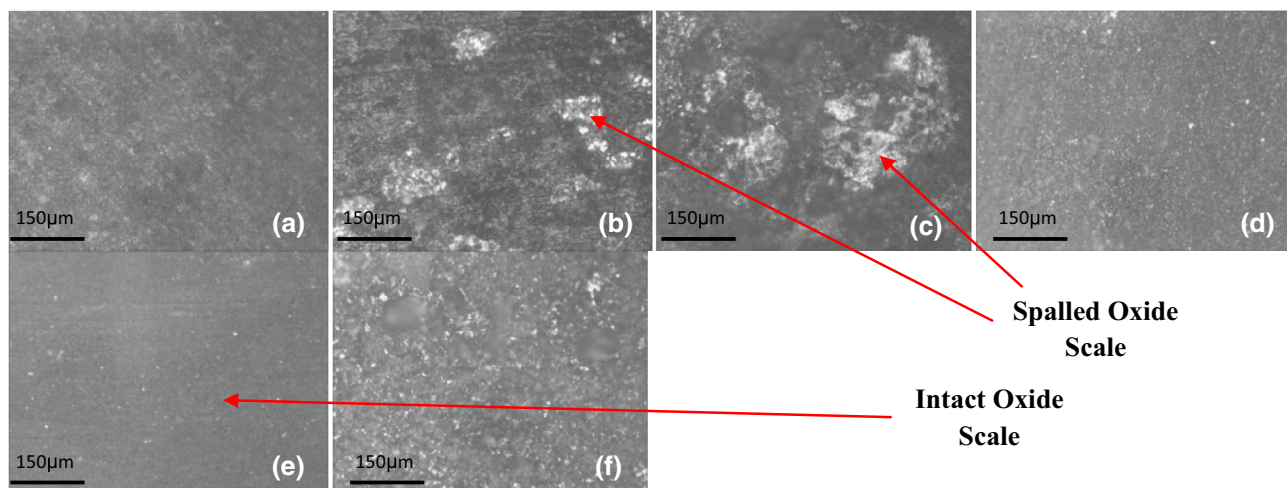


Fig. 2 Micrograph of nickel-base superalloys exposed to oxidation tests for 27 cycles, at 900, 1000 and 1100 °C ($\times 250$): **a, b** oxidized Inconel 600, respectively, **d, e, f** oxidized Hastelloy C-22, respectively

3 Results and Discussion

The results of high-temperature oxidation was included: (a) the experimental work results of the cyclic oxidation behavior of studied alloys and (b) the theoretical modeling which had been achieved by p-kp model.

3.1 Microstructural examination

Obviously, both alloys (Inconel 600 & Hastelloy C-22) after completion of the cyclic oxidation tests showed a good tendency to develop a uniform oxide scale coated all the alloy surfaces from the initial cycles of the air oxidation and at different exposure condition that included oxidation at different temperatures. In general, all the specimens showed a good adherence of the oxide film after or during the course of cyclic oxidation.

However, the oxide film formed on specimen surfaces that oxidized at 1100 °C suffered severe spallation behavior. Figure 2 reveals the degree of the scale spallation for both alloys in a form of white spots which represented the bare metal after the oxide scale spalled and black spot represents the intact oxide scale on the alloy surface. This spallation generated may be due to high internal stresses induced by oxide thickening and relatively during the cooling stage.

From Fig. 3a, b of etched specimens oxidized at 1100 °C, continuous oxide layer is visible. Obviously that the thickness of the external oxide layer increased with the temperature increase in cyclic oxidation. According to the kinetics results, observation can predicate absolutely the internal oxidation behavior in our study, but the current transverse microstructure results can show a little internal oxidation clue without any presence of diffusion layer could be observed.

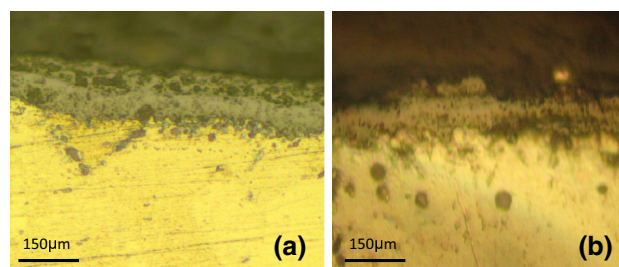


Fig. 3 Transverse section for nickel-base superalloys after cyclic oxidation tests at 1100 °C, ($\times 250$): **a** Inconel 600, **b** Hastelloy C-22

The microstructures of superalloys were usually typified by an austenitic face-centered cubic matrix phase known as gamma (γ) and variety of secondary phases. As seen in Fig. 4a, e, the grain boundaries were clearly observed with fine grains showed in Inconel 600 and coarse grains in Hastelloy C-22 and without second phase present in both alloys. Also twining was clearly evident in both alloys. As seen in Fig. 4a, e, the grain boundaries were clearly observed with fine grains showed in Inconel 600 and coarse grains in Hastelloy C-22 and without second phase present in both alloys. Also twining was clearly evident in both alloys. After cyclic oxidation tests, the present study validates the researches that showed that the oxidation of Hastelloy C-22 at 900 °C increases the number of precipitates within grains as well as thickening of grain boundary precipitates as shown in Fig. 4f. The type of precipitate was not detected by XRD technique, but Mori [7] had shown that these precipitates are Mo–W-mixed carbides of the types $(\text{Mo,W})_6\text{C}$ and Talekar [16] had confirmed that there is a definite formation of grain boundary precipitates with according to EDS line scans along the grain boundary precipitates revealed the presence of higher concentrations of molybdenum and lower concentrations of

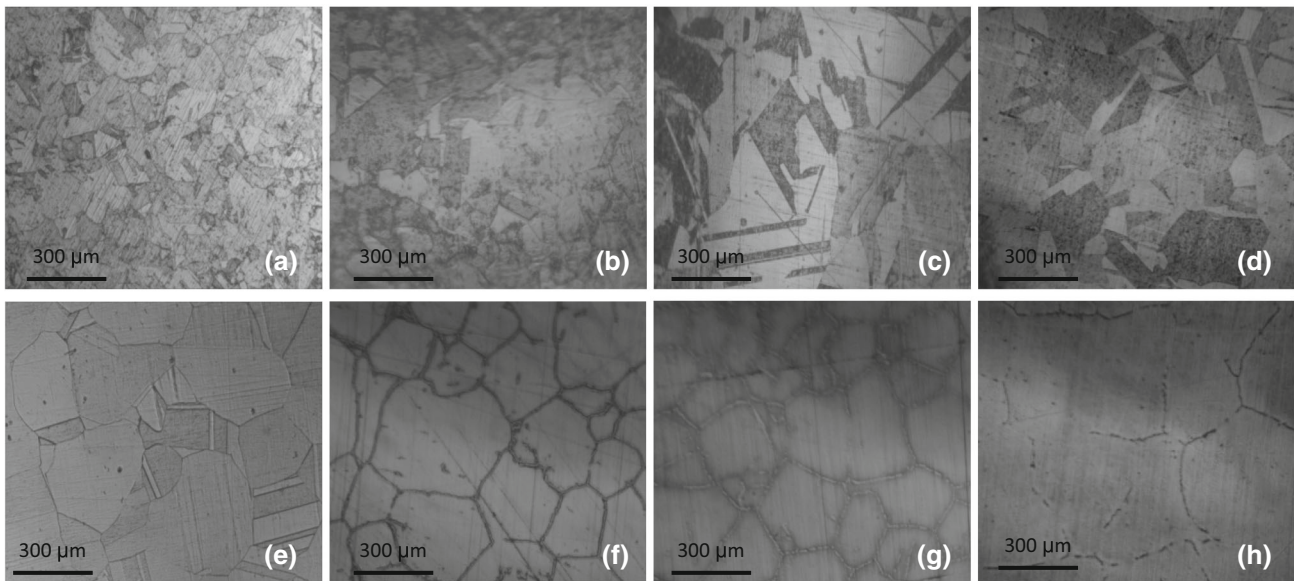


Fig. 4 Micrograph showing grain structure of nickel-base alloys before and after cyclic oxidation tests ($\times 125$): Inconel 600: **a** as received, **b** at 900°C, **c** at 1000°C, **d** at 1100°C; Hastelloy C-22: **e** as received, **f** at 900°C, **g** at 1000°C, **h** at 1100°C

Cr and Ni. Mori had mentioned that the amount of precipitated grain boundary carbides decreases when temperature increase from 1000 to 1100°C and that was also confirmed in our study as shown in Fig 4g, h. These precipitates were not present in Inconel 600 after completing all the cyclic oxidation testing from 900 to 1100°C. The grains of both alloys were also showed increasing in size with increasing the temperature of oxidation.

3.2 Weight Change Measurements

The cyclic oxidation experiments were performed on Inconel 600 and Hastelloy C-22 at temperatures range from 900 to 1100°C up to 27 cycles at the same conditions of heating and cooling to ensure obtaining consistent results so that the comparison between the studied alloys is possible.

Figures 5, 6 and 7 show the comparative results of measurement of specific weight change between Inconel 600 and Hastelloy C-22.

It is obvious from the plot that both alloys at 900 and 1000°C showed slight difference in the weight gain results, in spite of Hastelloy C-22 exhibited higher weight gain at initial cycles which is known as *transient oxidation*, occurs for almost all alloy systems for which the oxides of more than one component have negative free-energy changes for their formation in the given atmosphere [18], this is shown schematically for the transition from internal to external oxidation of Cr element, which forms a more stable oxide than Ni element but where some NiO forms before Cr_2O_3 becomes continuous. The extent of the transient period is decreased by those factors which promote selective oxidation, so observed

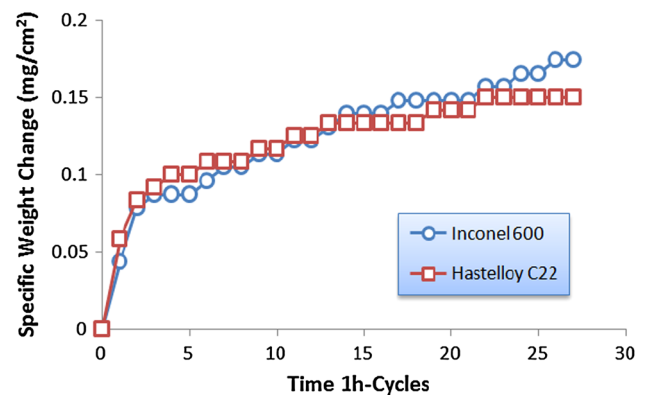


Fig. 5 Specific weight change of Inconel 600 and Hastelloy C-22 during the cyclic oxidation at 900°C

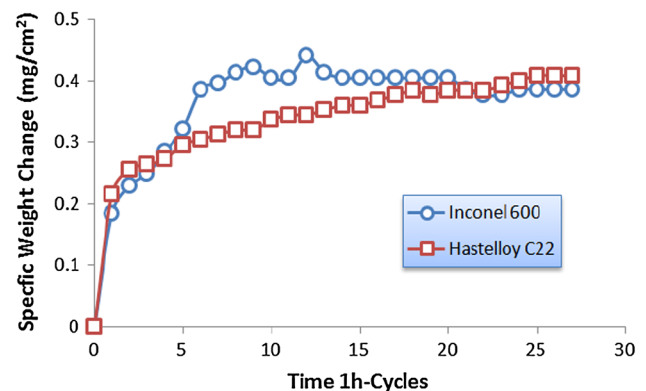


Fig. 6 Specific weight change of Inconel 600 and Hastelloy C-22 during the cyclic oxidation at 1000°C

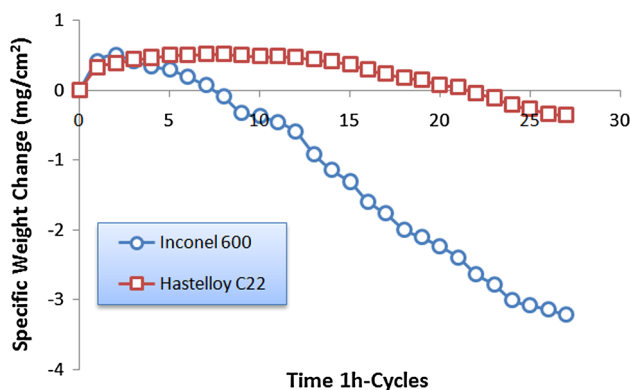


Fig. 7 Specific weight change of Inconel 600 and Hastelloy C-22 during the cyclic oxidation at 1100 °C

in Ni–Cr alloys the Ni-rich oxide is less ability to form in high Cr content alloys. Cr content in Hastelloy C-22 is less than in Inconel 600 ;for this reason, Hastelloy C-22 showed a *transient* stage in the early stage of high-temperature oxidation behavior.

At 1100 °C, both alloys showed two stages in the curve, the first stage included an increase in the weight of specimens which was due to the oxide formation. In the second stage, the alloys showed a noticeable decrease in the weight gain, and the slope of weight gain per unit area versus time falls to zero and then becomes negative after maximum $\Delta W/A$ value achieved and the curves become nearly linear. The magnitude of spallation was related to the downward slope of the weight gain curves.

In general, the oxidation kinetics of both alloys followed nearly the parabolic behavior during oxide formation as shown during all experiments. It is important to refer that

the weight changing at 900 °C was very slow and very low. The proof of that showed in numbers of identical consecutive data points with no gain, this is because of the specimen area was relatively small, and subjected time was short.

As a matter of fact that the chromia oxide cannot work in temperature condition greater than 1000 °C so with our studied alloy which they belong to chromia former alloys unlikable to use them in environments conditions as has been experimented and if we will go to use these alloys with oxidation temperatures beyond 1100 °C it will lead may to reduce the parabolic behavior and the materials going in their kinetic under only the linear oxidation behavior.

3.3 X-Ray Diffraction Analysis

To obtain information on the type of oxide scale formed, XRD technique was used. XRD analysis was carried out using X-ray diffractometer, X' Pert Pro MPD, PANalytical Co., Netherlands, with Cu K α radiation 1.54060 Å, and XRD database of JCPDS-ICDD for "International Center for Diffraction" data also was used with XRD Qualitative Analysis program version 1.0 to make matching between our results and the database.

As mentioned before, Ni-base superalloys are categorized as predominantly alumina (Al₂O₃) or predominantly chromia (Cr₂O₃) formers. Both of the Ni-base alloys used in this study are predominatly chromia formers as can be seen from their composition. Figures 8 and 9 show the XRD spectra for both alloys before and after the cyclic oxidation tests. In all cases, peaks that appeared from XRD analysis correspond to Cr₂O₃ and some of spinal oxide NiCr₂O₄ which were detected already after each test for all investigated oxide

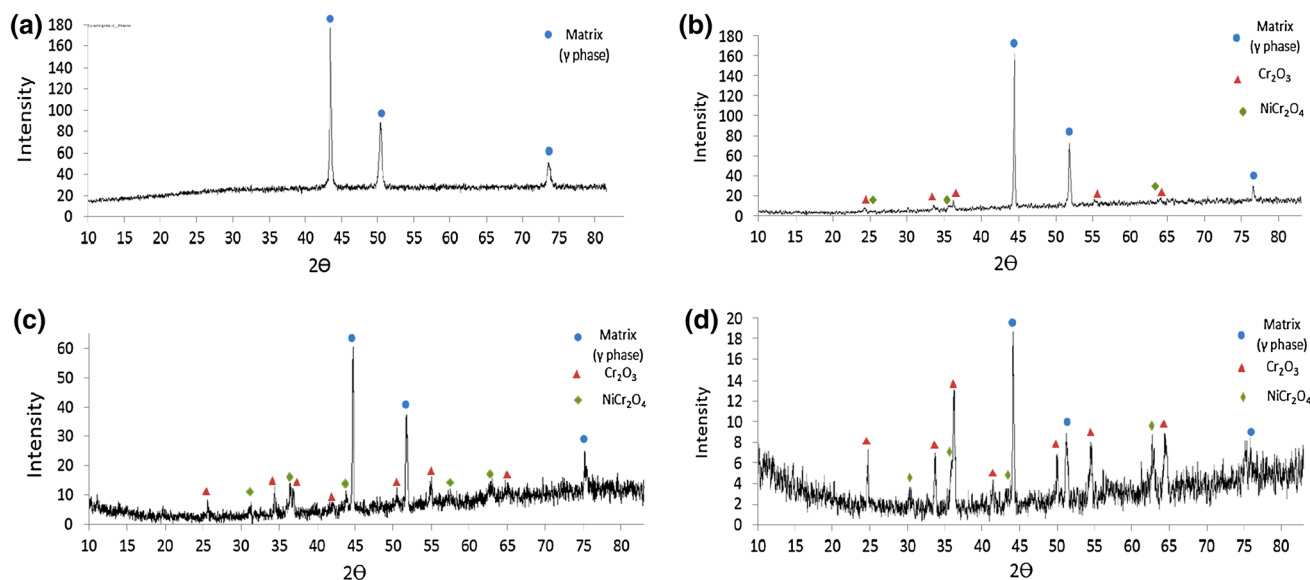


Fig. 8 XRD patterns for Inconel 600 before and after cyclic oxidation for 27 cycles: **a** as received **b** at 900 °C, **c** at 1000 °C, **d** at 1100 °C

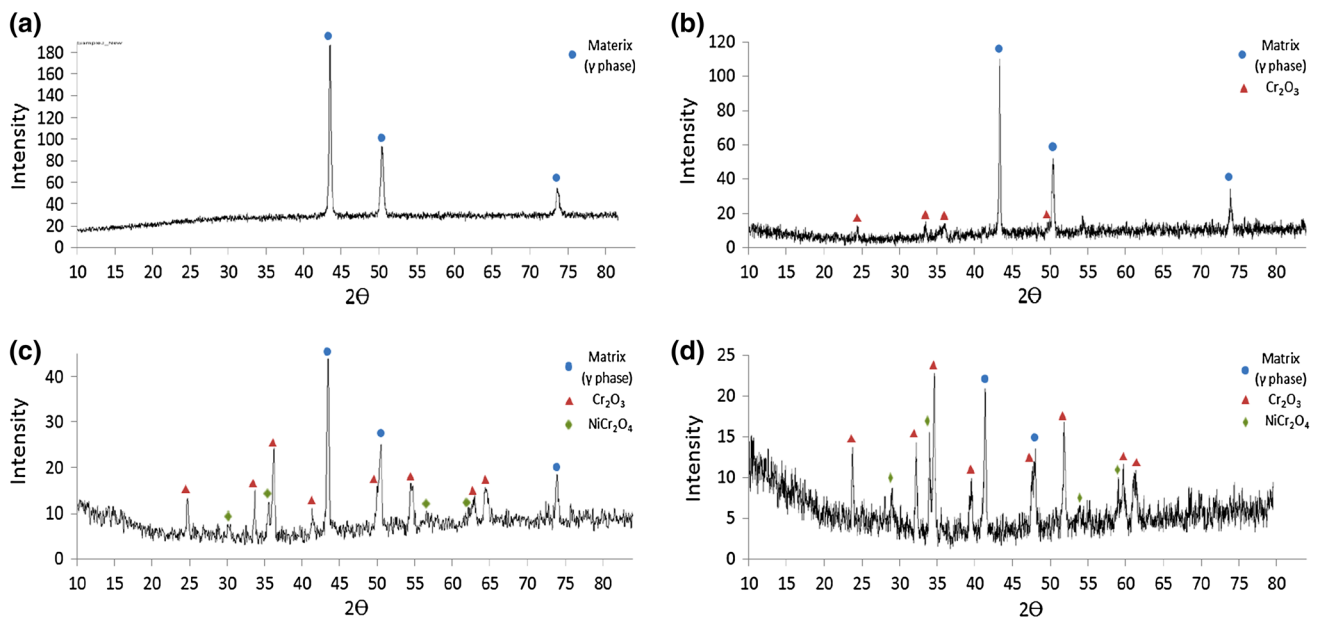


Fig. 9 XRD patterns for Hastelloy C-22 before and after cyclic oxidation for 27 cycles: **a** as received, **b** at 900°C, **c** at 1000°C, **d** at 1100°C

Table 2 Results of simulation and determination of p-kp model parameters

| Alloys | Temperature (°C) | p | $kp(\text{mg}^2/\text{cm}^4 \cdot \text{s})$ | $\Delta t(\text{hr})$ | $A(\sqrt{kp\Delta t})$ | C_m | C_0 | $F(p, kp)$ |
|----------------|------------------|--------|--|-----------------------|------------------------------|-------|-----------|------------|
| Inconel 600 | 900 | 0.0057 | 5.1×10^{-7} | 1 hr | $4.3 \text{ times } 10^{-2}$ | – | – | 0.00145 |
| | 1000 | 0.0128 | $7.9 \text{ times } 10^{-6}$ | | $1.7 \text{ times } 10^{-1}$ | 15 | – | 0.0102 |
| | 1100 | 0.0794 | $4.3 \text{ times } 10^{-5}$ | | $3.9 \text{ times } 10^{-1}$ | 2 | $\cong 7$ | 0.4265 |
| Hastelloy C-22 | 900 | 0.0051 | $4.3 \text{ times } 10^{-7}$ | | $3.9 \text{ times } 10^{-2}$ | – | – | 0.0037 |
| | 1000 | 0.0093 | $5.3 \text{ times } 10^{-6}$ | | $1.4 \text{ times } 10^{-1}$ | – | – | 0.0259 |
| | 1100 | 0.0284 | $3.0 \text{ times } 10^{-5}$ | | $3.3 \text{ times } 10^{-1}$ | 9 | 24 | 0.0164 |

scales on Inconel 600 and Hastelloy C-22, No signal for NiO was detected, which may be due to the small thickness and cannot be detected by XRD.

3.4 Simulation of p-kp Model

In the present study, the simulation of the cyclic oxidation behavior for both alloys was carried out by p-kp model. The p-kp model applied when oxide growth follows the parabolic kinetics during successive high-temperature isothermal oxidations. During the cooling, the oxide scale partly spalls. The spalling is characterized through a probabilistic approach. This model depends on two constant contribution p (spalling probability) and kp (parabolic constant) which was used to determine the cyclic oxidation criteria, and these parameters control the alloy elements consumption rate and the oxide scale thickness or weight gain [13]. In general, for chromia-forming materials and according to the mathematical base of model, the following equations can use them to describe the oxidation behavior:

$$\text{Met}_n = \text{Met}_{n-1} - \frac{52}{48} \Delta M_n \quad (2)$$

$$\text{Ox}_n^{\text{ad}} = (1 - p) \left(\text{Ox}_{n-1}^{\text{ad}} + \frac{152}{48} \Delta M_n \right) \quad (3)$$

Then,

$$\text{NMG}_n = \text{Met}_n + \text{Ox}_n^{\text{ad}} \quad (4)$$

where Met_n is metal-mass modification, ΔM_n is total oxygen mass gain per unit sample area, Ox_n^{ad} is mass of adherent oxide, and NMG_n is net mass gain for n (number of oxidation cycles). Ratio 152/48 is the molecular weight of Cr_2O_3 oxide to oxygen, and ratio 52/48 is relevant to molecular weight of chromium to oxygen, i.e., metal to oxygen ratio. Usually, the available experimental data are NMG_n , so the comparison between the experimental data and model data depends on this quantity. The power of this model can be computed very easily with numerical program using the "Microsoft Excel Program." The error function $F(p, kp)$ was introduced in order to minimize the deviation or the difference between

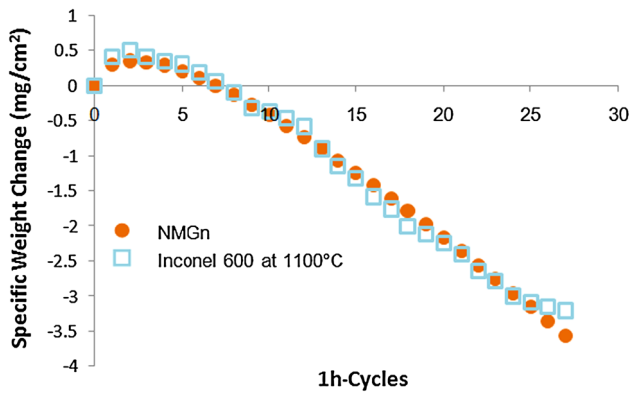


Fig. 10 Comparison of p-kp model fits with actual cyclic data for Inconel 600 at 1100°C with 1-h cycles

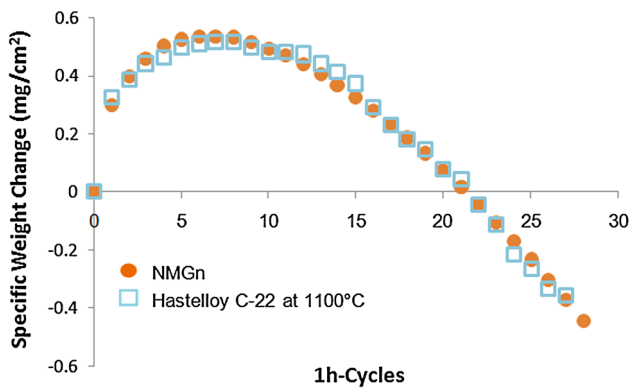


Fig. 11 Comparison of p-kp model fits with actual cyclic data for Hastelloy C-22 at 1100°C with 1-h cycles

the calculated and experimental data. The fitting procedure was conducted to find the couple (p,kp) through the minimization of the error function using Microsoft Excel solver. After completed the simulation of cyclic oxidation for both alloys, the model parameters are displayed in Table 2 with the minimum error function that is given by fitting program (by Microsoft Excel).

Figures 10 and 11 show the experimental results of Inconel 600 and Hastelloy C-22 during the cyclic oxidation at 1100°C with net mass gain NMG_n curves of p-kp model. The model curves are in fairly good agreement with experimental values. These curves give the general trend of the kinetics for Inconel 600 and Hastelloy C-22 subjected to cyclic oxidation tests.

It should be noted that when experimental data contain both points C_m and C₀, the comparison between the fitted model and experimental data is generally good. In the case of Inconel 600 and Hastelloy C-22 both oxidized at 900°C, the NMG_n curve corresponds to “pseudo-parabolic” kinetics with no maximum, in that case p approximately equals to zero and the model is not relevant. However, the values of kp for both alloys were compatible with different

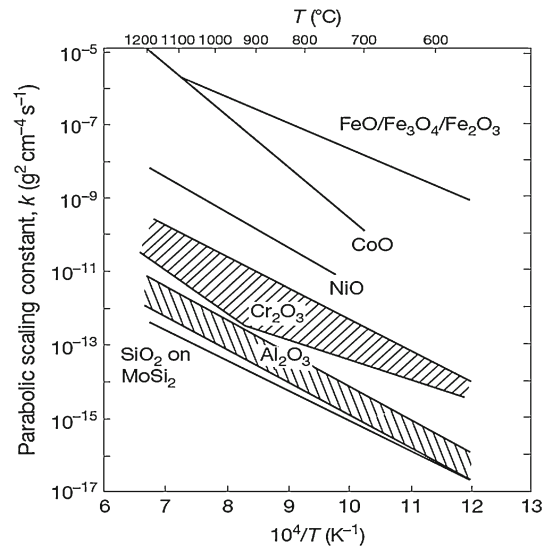


Fig. 12 Parabolic oxidation rate constant for various oxide scales as a function of temperature [17]

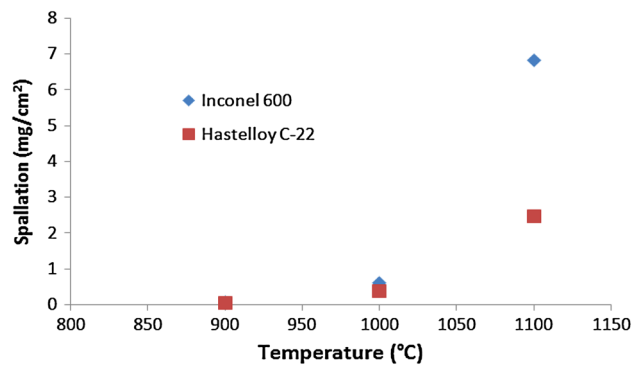


Fig. 13 Effect of temperature on the spallation behavior on Inconel 600 and Hastelloy C-22

researches [7, 15, 16] and were in good agreement with data of chromia-forming alloys which can be seen in Fig. 12 [17]. According to the model used, in all cases, the amount of spallation of Inconel 600 was found to be larger than that of Hastelloy C-22 as shown in Fig. 13. That was expected through examining the values of spalling probability, where the values of p obtained from the model to Inconel 600 were found to be greater than the values of Hastelloy C-22. The p-kp oxidation life map was plotted as shown in Fig. 14. From the oxidation life map, it was observed that most of the results were related to oxidation temperature above 1000°C lying between the poor adherence region and the fast-growth region. These data clearly demonstrated that Hastelloy C-22 had features of better cyclic oxidation resistance and also showed that properties of oxidation resistance increased with the decrease in oxidation temperature.

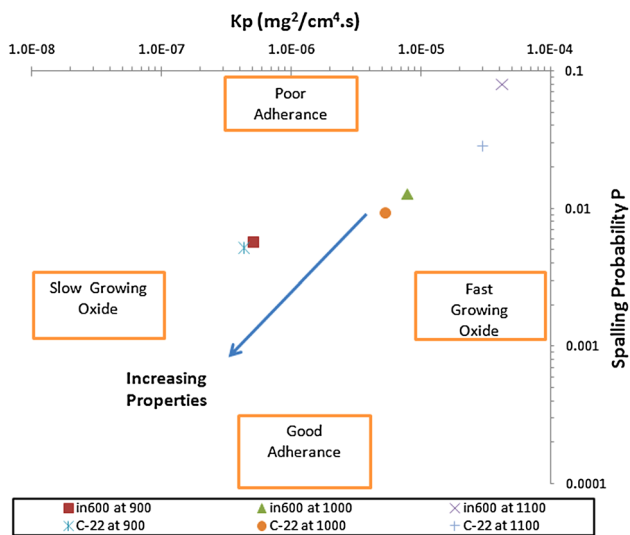


Fig. 14 P-kp oxidation life map showed the performance of Inconel 600 and Hastelloy C-22

4 Conclusions

1. Inconel 600 and Hastelloy C-22 showed a good tendency to develop a uniform chromia oxide scale coated the outer surfaces from the initial cycles of the high-temperature oxidation and at different temperatures. Smaller amounts of spinel oxides were also observed.
2. The oxidation kinetics of both alloys followed nearly the parabolic behavior during oxide formation.
3. The oxide films for both alloys suffered severe spallation at 1100°C and confirmed that chromia oxide had no ability to work above 1000°C. The extent of spalling increased with increasing exposure temperature.
4. The p-kp model was successfully adapted to cyclic oxidation data obtained for Inconel 600 and Hastelloy C-22 describing the process of oxide growth and spallation. The model was used to make simplified lifetime predictions.
5. Prolonged exposure period of time for oxidation, the weight of the specimens could be approximated as decreasing linearly with time and the adherent oxide mass approached a constant value, as confirmed by the model.
6. The p-kp oxidation life map was plotted; the results data clearly demonstrated that Hastelloy C-22 had features of better cyclic oxidation resistance.

References

1. Askeland, D.R.: *The Science and Engineering of Materials*, 6th ed. Cengage Learning, Inc., Boston (2010)
2. Reed, R.C.: *The Superalloys Fundamentals and Applications*, 1st ed. Cambridge University Press, Cambridge (2006)
3. Cottis, R.A.: *Shreir's Corrosion*, 4th ed. Elsevier Ltd., New York (2010)
4. Smialek, J.L.: A deterministic interfacial cyclic oxidation spalling model. *Acta Materialia* **51**, 469–483 (2003)
5. Smialek, J.L.; Nesbitt, J.A.; Barrett, C.A.; Lowell, C.E.: *Cyclic Oxidation Testing and Modelling: A NASA Lewis Perspective*, National Aeronautics and Space Administration, Glenn Research Center, NASA/TM 1999-209769, (2000)
6. Huang, J.; Fang, H.; Fu, X.; Huang, F.; Wan, H.; Zhang, Q.; Deng, S.; Zu, J.: High-temperature oxidation behavior and mechanism of a new type of wrought Ni–Fe–Cr–Al superalloy up to 1300°C. *Oxid. Met.* **53**, 273–287 (2000)
7. Mori, G.: Oxidation of nickel base alloys strengthened by different hardening effects. *Corros. Eng. Sci. Technol.* **39**, 236–244 (2004)
8. Singh, H.; Puri, D.; Prakash, S.; Maiti, R.: Characterization of oxide scales to evaluate high temperature oxidation behavior of Ni–20Cr coated superalloys. *Mater. Sci. Eng. A* **464**, 110–116 (2007)
9. Xiao, J.; Prud'homme, N.; Li, N.; Ji, V.: Influence of humidity on high temperature oxidation of Inconel 600 alloy: oxide layers and residual stress study. *Appl. Surf. Sci.* **284**, 446–452 (2013)
10. Stiger, M.J.; Meier, G.H.; Pettit, F.S.; Ma, Q.; Beuth, J.L.; Lance, M.J.: Accelerated cyclic oxidation testing protocols for thermal barrier coatings and alumina-forming alloys and coatings. *J. Mater. Corros.* **57**, 73–85 (2006)
11. Lowell, C.E.; Barrett, C.A.; Palmer, R.W.; Auping, J.V.; Probst, H.B.: COSP: a computer model of cyclic oxidation. *Oxid. Met.* **36**, 81–112 (1991)
12. Smialek, J.L.; Auping, J.V.: COSP for windows-strategies for rapid analyses of cyclic-oxidation behavior. *Oxid. Met.* **57**, 559–581 (2002)
13. Poquillon, D.; Monceau, D.: Application of a simple statistical spalling model for the analysis of high-temperature, cyclic-oxidation kinetics data. *Oxid. Met.* **59**, 409–431 (2003)
14. N'Dah, E.; Tsipas, S.; Hierro, M.P.; Perez, F.J.: Study of the cyclic oxidation resistance of Al coated ferritic steels with 9 and 12% Cr. *Corros. Sci.* **49**, 3850–3865 (2007)
15. Singh, H.; Puri, D.; Prakash, S.; Maiti, R.: Characterization of oxide scales to evaluate high temperature oxidation behavior of Ni–20Cr coated superalloys. *Mater. Sci. Eng. A* **464**, 110–116 (2007)
16. Talekar, A.S.: Oxidation behavior of Ni-base superalloys and high strength low alloy (Hsla) steels at elevated temperatures. Ph.D. thesis, University of Nevada, Reno, (2008)
17. Gleeson, B.: *Corrosion and environmental degradation*, vol. II. In: Schutze, M. (ed.) *The Materials Science and Technology Series*, vol. 19, Wiley-VCH, Weinheim (2000)
18. Birks, Neil; Meier, Gerald, H.; Pettit, Fred, S.: *Introduction to the High-Temperature Oxidation of Metals* 2nd ed. Cambridge University Press, Cambridge (2006)